Effects of Mutations near the Bacteriochlorophylls in Reaction Centers from *Rhodobacter sphaeroides*†

J. C. Williams, R. G. Alden, H. A. Murchison, J. M. Peloquin, N. W. Woodbury, and J. P. Allen*

Department of Chemistry and Biochemistry, and Center for the Study of Early Events in Photosynthesis, Arizona State University, Tempe, Arizona 85287-1604

Received February 25, 1992; Revised Manuscript Received August 12, 1992

ABSTRACT: Mutations were made in four residues near the bacteriochlorophyll cofactors of the photosynthetic reaction center from *Rhodobacter sphaeroides*. These mutations, L131 Leu to His and M160 Leu to His, near the dimer bacteriochlorophylls, and M203 Gly to Asp and L177 Ile to Asp, near the monomer bacteriochlorophylls, were designed to result in the placement of a hydrogen bond donor group near the ring V keto carbonyl of each bacteriochlorophyll. Perturbations of the electronic structures of the bacteriochlorophylls in the mutants are indicated by additional resolved transitions in the bacteriochlorophyll absorption bands in steady-state low-temperature and time-resolved room temperature spectra in three of the resulting mutant reaction centers. The major effect of the two mutations near the dimer was an increase up to 80 mV in the donor oxidation–reduction midpoint potential. Correspondingly, the calculated free energy difference between the excited state of the primary donor and the initial charge separated state decreased by up to 55 mV, the initial forward electron-transfer rate was up to 4 times slower, and the rate of charge recombination between the primary quinone and the donor was ~30% faster in these two mutants compared to the wild type. The two mutations near the monomer bacteriochlorophylls had minor changes of 25 mV or less in the donor oxidation–reduction potential, but the mutation close to the monomer bacteriochlorophyll on the active branch resulted in a roughly 3-fold decrease in the rate of the initial electron transfer.

The primary process in photosynthesis occurs in a pigment–protein complex termed the reaction center [reviewed in Kirmaier and Holten (1987), Feher et al. (1989), and Parson (1991)]. The reaction center from *Rhodobacter sphaeroides* wild-type strain 2.4.1 contains three subunits (L, M, and H), a bacteriochlorophyll (Bchl)[1] dimer (P), two bacteriochlorophyll monomers (B), two bacteriopheophytin (Bphe) monomers (H), two ubiquinones (Q), a carotenoid, and a nonheme Fe^{2+}. The cofactors are divided into two symmetrical branches labeled A and B. Light energy, absorbed by the light-harvesting complexes of the photosynthetic membrane, is transferred to the Bchl dimer of the reaction center. Within the next 3–4 picoseconds (ps), electron transfer takes place from the excited singlet state of P (P*), ultimately forming the charge separated state $P^+H_A^-$. The electron is transferred from H_A^- to the primary quinone, Q_A, in approximately 200 ps, and then from Q_A^- to Q_B in hundreds of microseconds. The back-reaction times are all at least an order of magnitude slower than the forward times, thus the quantum yield is near unity. There is apparently little or no electron transfer from P to H_B.

Several groups have developed and utilized systems for site-directed mutagenesis of reaction centers (Youvan et al., 1985; Farchaus & Oesterhelt, 1989; Paddock et al., 1989; Nagarajan et al., 1990; Takahashi et al., 1990). Using these systems, a number of reaction center mutations in the vicinity of P, the monomer Bchls, and the Bphes have been produced, initiating a new approach to the study of the initial electron-transfer mechanism (Coleman & Youvan, 1990; Finkele et al., 1990; Nagarajan et al., 1990; Schenck et al., 1990; Woodbury et al., 1990; Chan et al., 1991; Kirmaier et al., 1991). Measurements on mutant reaction centers have shown that the spectral characteristics and electron-transfer rates can be altered by changing specific amino acid residues.

One of the outstanding questions of the reaction center structure–function relationship is how each of the four Bchls is involved in the primary process of electron transfer. To address this question, we have designed modifications of the reaction center to introduce hydrogen bonds to the 9-keto groups of each Bchl. The addition of a hydrogen bond to the keto group should perturb the electronic structure of the specific Bchl. These changes were patterned after the hydrogen bonding of Glu L104 to H_A, which is principally responsible for the difference in the Q_x transition energies of H_A and H_B, resulting in two distinct optical absorption bands at 532 and 545 nm (Bylina et al., 1988). We report the characterization of the altered optical spectra, energy levels, and electron transfer rates for the four mutants.

METHODS

Design of Mutants. A set of mutations in the reaction center has been made in which residues near each Bchl were replaced with another amino acid that could possibly form a hydrogen bond to the 9-keto carbonyl of ring V, subject to the constraints of the structure (Table I). Since this carbonyl is part of the conjugation system, the formation of a hydrogen

† This work was supported by Grants GM41300 and GM45902 from the National Institutes of Health, Grants DMB89-177729 and DMB91-58251 from the National Science Foundation, and Postdoctoral Fellowship in Plant Biology DIR-9104322 from the National Science Foundation. Instrumentation was purchased with funds from NSF Grant DIR-8804992 and DOE Grants DE-FG-05-88-ER75443 and DE-FG-05-87-ER75361. This is publication No. 107 from the Arizona State University Center for the Study of Early Events in Photosynthesis. The Center is funded by DOE Grant DE-FG-88-ER13969 as a part of the USDA/DOE/NSF Plant Science Centers Program.

[1] Abbreviations: Bchl, bacteriochlorophyll; Bphe, bacteriopheophytin; P, Bchl dimer; B, Bchl monomer; H, Bphe monomer; Q, quinone; ps, picosecond; EDTA, (ethylenedinitrilo)tetraacetic acid; Tris, tris(hydroxymethyl)aminemethane.

0006-2960/92/0431-11029$03.00/0

Table I: Mutations Designed To Introduce Hydrogen Bonds to Reaction Center Bacteriochlorophylls

mutant	change	nearest cofactor
LH(L131)	L131 Leu to His	P_A
LH(M160)	M160 Leu to His	P_B
GD(M203)	M203 Gly to Asp	B_A
ID(L177)	L177 Ile to Asp	B_B

bond will alter the electronic structure of the Bchl. Potential changes in the three-dimensional structure due to substituting each residue were examined using an Iris graphics workstation (Silicon Graphics) and the program QUANTA. Substitutions of residues within 10 Å of the targeted carbonyl oxygen by amino acids with an oxygen or nitrogen that could serve as a donor in a hydrogen bond were made to determine which changes would most likely result in a hydrogen bond distance of approximately 3 Å with the proper orientation. For each case, the side chain was replaced and the resulting geometry was manually adjusted to determine side chain locations that had minimal steric interactions with other residues. For the dimer Bchls, P_A and P_B, residue Leu L131 and the symmetry-related residue Leu M160 were found to yield the most promising substitutions when replaced with histidine (Figure 1). For the monomers B_A and B_B, similar analysis suggested the replacement of Gly M203 with an aspartic acid residue and replacement of Ile L177 with an aspartic acid residue, respectively. The residues Leu L131 and Leu M160, in addition to being near P_A and P_B, respectively, are within 5 Å of the nearby monomers, B_A and B_B, respectively. Similarly, residue Ile L177 is within 5 Å of P_A. The residue Gly M203 is farther than 8 Å from all cofactors other than B_A of the reaction center.

Construction of Mutants. The genes encoding the L and M subunits, *puf*L and *puf*M, are part of the *puf* operon, which also includes *puf*Q, encoding a protein involved in bacteriochlorophyll synthesis; *puf*A and *puf*B, encoding subunits of the B875 light-harvesting complex; and *puf*X, an open reading frame whose function has not been elucidated [reviewed in Scolnik and Marrs (1987) and Kiley and Kaplan (1988)]. The mutagenesis system for *puf*L and *puf*M is a modification of that described by Paddock et al. (1989) for making specific changes in residues in the L subunit, and it has been used successfully to introduce a number of mutations in the *puf*L and *puf*M genes (J. C. Williams, M. L. Paddock, G. Feher, and J. P. Allen, unpublished results). For oligonucleotide-directed mutagenesis, fragments of the genes were subcloned into M13 phage derivatives (Yanisch-Perron et al., 1985). Oligonucleotide-directed mutagenesis based upon the modification of Sayers et al. (1988) or Tsurushita et al. (1988) was used with approximately 50% efficiency. The presence of the mutation and the fidelity of the remaining DNA were verified by dideoxy sequencing for each mutation. After alteration of the genes on the small subcloned fragments, the *puf* operon was reassembled in the broad host range plasmid pRK404 (Ditta et al., 1985) into which a 4.3 kilobase pair *Eco*RI–*Nru*I fragment that contains the *puf* operon was cloned. The plasmid containing the reconstructed *puf* operon was then introduced by conjugation into *Rb. sphaeroides* strain ΔLM1.1, in which the wild-type reaction center *puf*L and *puf*M genes on the chromosome have been deleted (Paddock et al., 1989).

The complemented *Rb. sphaeroides* strains were grown semiaerobically on rich media for isolation of reaction centers following protocols developed for the wild-type 2.4.1 strain (Paddock et al., 1989). After isolation, the reaction center buffer consisted of 15 mM Tris-HCl, pH 8, 1 mM EDTA, and 0.025% lauryldimethylamine *N*-oxide. For the redox titrations and the fast transient fluorescence spectroscopy, the buffer was changed to 100 mM Tris-HCl, pH 8, 1 mM EDTA, and 0.05% Triton X-100. For all experiments, wild-type reaction centers were those isolated from the deletion strain complemented with the wild-type genes.

Low Temperature Optical Spectroscopy. Samples ($A_{802}^{1\,cm} \sim 3 - 4$) were diluted with 2 vol of glycerol. After thorough mixing, air bubbles were removed by centrifugation for 3 min at 4000 rpm. Samples were cooled to cryogenic temperatures using a 1.5-mm pathlength sample holder with quartz windows mounted to the cold tip of a helium displex refrigerator (APD). Temperatures were maintained using a thermofoil heater (Minco) attached to the cold tip and were monitored using a calibrated Cu–Au thermocouple. Both heater and thermocouple were controlled using a Series 8000 temperature controller (APD). The refrigerator was mounted in the sample compartment of a Cary 5 spectrophotometer (Varian). All measurements were taken versus air in the reference compartment of the spectrophotometer. The slew rate was 1 nm/s, and the visible to infrared detector change was set at 680 nm. To the blue of the detector change the spectral band width was 2.00 nm while to the red it was 2.50 nm. The spectral bandwidth was kept constant while the gain of the detector was varied automatically by the instrument. Two baseline corrections were performed on the spectra. All spectra were corrected so as to have an absorbance of 0 at 1000 nm. The region of the spectra to the blue of 680 nm was corrected to remove an offset caused by the detector change.

Transient Fluorescence Spectroscopy. Samples consisted of reaction centers ($A_{802}^{1\,cm} \sim 1.8$) to which 10 mM sodium dithionite was added to reduce the primary quinone. Transient fluorescence spectra were measured in a 0.15-cm cuvette by single photon counting in an apparatus that has been previously described (Gust et al., 1990) by methods detailed in Taguchi et al. (1992). Excitation was at 860 nm with 10-ps pulses, and emission was measured at wavelengths ranging from 880 to 940 nm.

Redox Titrations. Reaction centers ($A_{802}^{1\,cm} \sim 0.5$, vol ~ 10 mL) were placed into a flow cell with an external mixing chamber. The ambient redox potential and the optical absorbance spectrum were measured simultaneously. The redox potential was measured with a platinum electrode and calomel reference electrode. The electrodes were calibrated using equimolar ferri/ferrocyanide mixtures in various pH buffers (O'Reilly, 1973). A similar calibration was obtained using quinhydrone. The potential was adjusted by the addition of potassium ferricyanide or ascorbic acid. The optical spectrum from 750 to 1000 nm was measured at each potential on a Cary 5 spectrophotometer. The spectra were normalized to the Bchl absorption peak near 800 nm to correct for degradation of the reaction centers during the titration. Upon oxidation, the absorption peak at 802 nm shifts several nanometers to the blue and increases approximately 3% in amplitude compared to the fully reduced amplitude. This amplitude change causes an error of less than 2 mV in the calculated midpoint potential. The fraction of the reaction centers that was reduced was determined by comparing the normalized absorbance at 865 nm to the maximum absorbance at 865 nm (100% reduced) and the minimum absorbance at 865 nm (0% reduced). The minimum absorbance of the dimer band was determined by measuring the spectrum in the

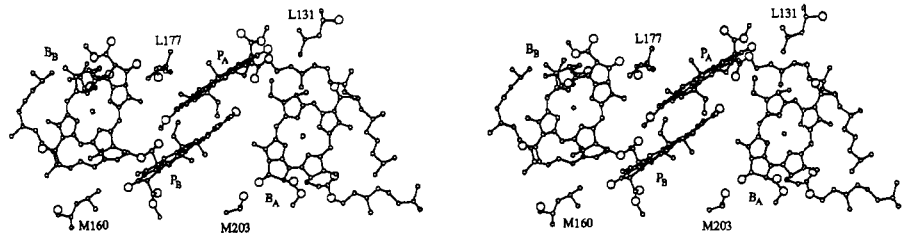

FIGURE 1: Stereo view of the dimer Bchls (P_A and P_B) and nearby residues Leu L131 and Leu M160 and the monomer Bchls (B_A and B_B) and nearby residues Gly M203 and Ile L177 of the wild-type reaction center structure of *Rb. sphaeroides*. For each Bchl, the nearest carbon of the targeted residue is within 4 Å of the 9-keto carbonyl of ring V. The view is down the 2-fold symmetry axis of the reaction center. Coordinates are from the Brookhaven National Laboratory Data Bank, file 4RCR (Allen et al., 1987a; Yeates et al., 1988).

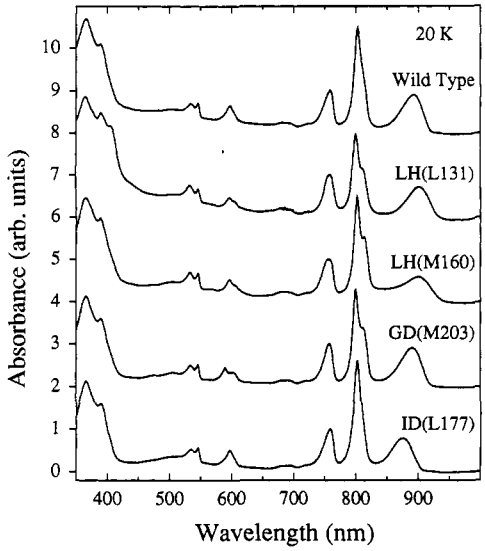

FIGURE 2: Low-temperature (20 K) optical absorption spectra of mutant reaction centers compared to the wild type. The spectra are normalized at 760 nm. Additional resolved transitions at 600 and 800 nm are observed in the spectra of three of the mutants compared to the wild type. The band at 890 nm in the spectrum of the wild type shifts 10 nm to the red in the spectra of the LH(L131) and LH(M160) mutants and 10 nm to the blue in the ID(L177) mutant.

presence of a saturating light source. The data were fit to the Nernst equation (n = 1).

Transient Absorption Spectroscopy. The rate of charge recombination from $P^+Q_A^-$ was measured on a flash spectrophotometer of local design. A 10-μs xenon flash lamp was used for excitation of samples. The change in absorbance was measured at 865 or 850 nm. Terbutryne (0.5 mM) was added to the reaction centers ($A_{802}^{1\,cm} \sim 0.5$) to block electron transfer from Q_A to Q_B. The data were fit to a single exponential.

The rates of the initial electron-transfer events were measured using a pulse–probe transient absorption apparatus (Taguchi et al., 1992). Spectra were measured with a dual diode array (Princeton Instruments) at a resolution of approximately 3 nm between 730 and 965 nm, after excitation at 590 nm with an approximately 200-fs pulse. For some kinetic measurements, the excitation beam was modulated at 42 Hz and a phase lock-in amplifier (EG&G) was used to determine the change in the log of the ratio of the signals from two diodes.

RESULTS

Initial Characterization. All of the mutant strains designed to introduce hydrogen bonds to the Bchl cofactors were able to grow photosynthetically at rates comparable to the wild-type strain. Reaction centers could be isolated from all of the mutants in normal yields. The A_{280}/A_{800} ratio was ~1.2 for the purest mutant reaction centers, except those isolated from the LH(L131) mutant, in which the A_{280}/A_{800} ratio was ~1.6.

Optical Absorption Spectra. The room temperature spectra (data not shown) of reaction centers isolated from the mutants were not significantly different from that of the wild type, with the exception of the ID(L177) mutant, in which the Q_y peak of the Bchl dimer was shifted from 865 to 850 nm. Light-induced formation of P^+ in this mutant results in a cation band that is blue-shifted 10–15 nm from the 1250-nm absorption band observed in the wild type. A 10-nm red shift, to 1260 nm, was observed in the cation band of the LH(L131) and LH(M160) mutants, with an approximately 3-fold decrease in amplitude in the LH(M160) mutant. The P^+ cation band in the GD(M203) mutant is essentially the same as in the wild type.

In low-temperature (20 K) spectra, systematic changes are observed for the mutants (Figure 2). Two resolved bands, 15 nm apart, are observed in the absorption spectra at ~600 and 800 nm in the LH(L131), LH(M160), and GD(M203) mutant reaction centers. The dimer band, which is at 890 nm in reaction centers isolated from the wild-type strain, is shifted 10 nm to the red in the two mutants designed to add hydrogen bonds to the dimer, LH(L131) and LH(M160), and 10 nm to the blue in the ID(L177) mutant. Changes are also observed in the relative oscillator strengths of the different bands. For example, in the LH(L131) mutant, the absorption band at 800 nm has decreased relative to the band at 760 nm. The two Bphe absorption peaks at 532 and 545 remain unchanged in all five spectra, as does the position of the 760-nm Q_y band of the Bphe. The significant alteration in transition energies and shapes of the Bchl bands, but not the Bphe bands, is consistent with specific perturbations of the electronic structures of the Bchls.

Fluorescence Decay Measurements. Time-correlated single photon counting techniques were used to determine the fluorescence decay in the 880–940-nm region for quinone-reduced reaction centers from the wild type and each of the four mutants. Four exponential terms were required to adequately fit the data. The amplitudes (A_1–A_4) and characteristic lifetimes (τ_1–τ_4) of the four components for one set of spectra measured at 920 nm are shown in Table II. The relative amplitudes of the two slowest fluorescence components, A_3 and A_4, are much larger in the two mutants designed to affect the donor, LH(L131) and LH(M160), than in the wild type. Changes are also observed for some of the rates. The time constant of the first component, τ_1, is fastest in the wild type and slower in the mutants, although measurement of these values is limited by the time resolution of the apparatus (approximately 10 ps). The time constants of the second and third components, τ_2 and τ_3, are similar in the wild type and each of the mutants. For the time constant of the fourth component, τ_4, a faster value than wild type was measured for the LH(L131), LH(M160), and ID(L177)

Table II: Fast Transient Fluorescence Data[a]

sample	τ_1 (ps)	A_1	τ_2 (ps)	A_2	τ_3 (ps)	A_3	τ_4 (ps)	A_4
wild type	8.4	973	90.0	23.2	731	2.09	5120	1.41
LH(L131)	23.9	878	123	89.1	784	22.4	3180	10.0
LH(M160)	13.8	954	107	29.5	734	10.8	3240	5.64
GD(M203)	23.5	947	129	47.8	828	2.86	7250	2.02
ID(L177)	15.6	959	129	36.6	888	2.74	4660	2.07

[a] Excitation was at 860 nm and emission was measured at 920 nm. The fluorescence decay was fit by four exponential terms, and the amplitudes (A_1, A_2, A_3, A_4) were normalized so that their sum is 1000.

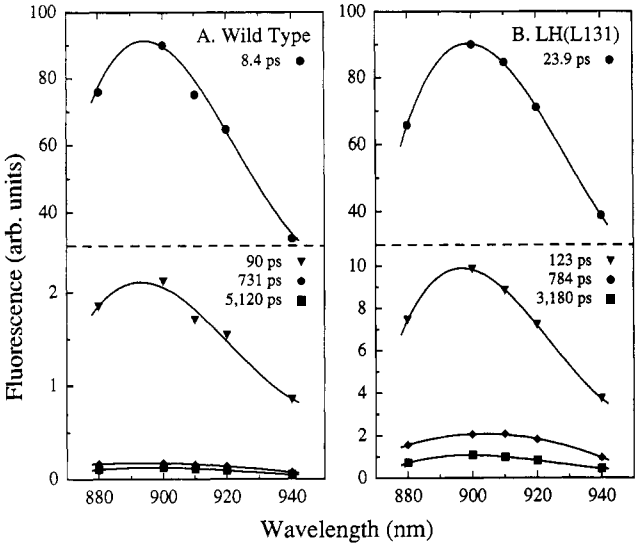

FIGURE 3: Decay-associated fluorescence spectra from reaction centers isolated from (A) the wild-type strain and (B) the LH(L131) mutant. Excitation was at 860 nm. The wavelength dependence of the amplitude is similar for the prompt and delayed components. The LH(L131) mutant shows an increase in amplitude of the delayed components relative to the wild type, indicating a decrease in the $P^*/P^+H_A^-$ free energy difference.

reaction centers, while a slightly slower value was measured for reaction centers from the GD(M203) mutant. Decay-associated spectra of the kinetic components of the fluorescence were determined for wild-type, LH(L131), and LH(M160) reaction centers. The LH(L131) mutant shows the same spectra of prompt and delayed components as the wild type (Figure 3), but in the LH(M160) mutant, the spectra are shifted to the red by approximately 10 nm for all four components (data not shown). A comparison of the amplitude of the prompt component to the sum of the amplitudes of the three delayed components provides an estimation of the standard free energy difference between P^* and $P^+H_A^-$ using an equilibrium model (Schenck et al., 1982; Woodbury et al., 1984; Taguchi et al., 1992). The amplitude of the prompt component was corrected for the limited time resolution of the instrument by the ratio of τ_1 to the P^* decay time as measured by femtosecond transient absorption spectroscopy (Taguchi et al., 1992). The calculated free-energy difference was decreased in all four mutants compared to wild type (Table III).

Midpoint Potential of P/P^+. The redox potentials of cofactors in proteins, such as the hemes in cytochromes, vary by several hundred millivolts, due to differences in ligations, the polarity of nearby residues, and other interactions (Poulos, 1987; Moore & Pettigrew, 1990). The introduction of hydrogen bonds to the dimer Bchls in reaction centers should preferentially stabilize the neutral state of P compared to the oxidized state and thus increase the P/P^+ redox midpoint potential. Redox titrations of reaction centers with mutations near the dimer are compared to wild-type reaction centers in Figure 4. The value of the midpoint potential of wild-type reaction centers was found to be approximately 495 mV, in agreement with results obtained using an electrochemical cell (Moss et al., 1991). The LH(L131) and LH(M160) mutants showed increases of approximately 80 and 55 mV, respectively, in their midpoint potentials relative to the wild type. The two mutations near the monomer Bchls did not show increases in their midpoint potentials, although the ID(L177) mutant showed a slight decrease. Reaction centers from the LH-(L131) and ID(L177) mutants were less stable under the titration conditions than those from the wild-type strain. The redox data are summarized in Table III.

$P^+Q_A^-$ Recombination Rates. The charge recombination rate of $P^+Q_A^-$ is sensitive to the standard free energy difference between $P^+Q_A^-$ and the ground state, PQ_A (Popovic et al., 1986; Feher et al., 1988; Gunner et al., 1989; Franzen et al., 1990). The introduction of hydrogen bonds to the Bchl dimer should alter the P/P^+ energy difference but not change the Q_A^- or Q_A energy levels. In the LH(L131) and LH(M160) mutants, which have an increased P/P^+ midpoint potential, the rate of $P^+Q_A^-$ charge recombination also increases (Table III). The rate of charge recombination in the GD(M203) mutant was similar to the wild type, but the rate decreased significantly in the ID(L177) mutant.

Femtosecond Time-Resolved Absorption Spectroscopy. Detailed comparison at various times after excitation reveals significant differences in the spectra of LH(L131) and wild-type reaction centers, especially in the 750–830-nm region (Figure 5). The initial (0.5 ps) excited state of LH(L131) reaction centers shows a large contribution from a species that bleaches at 800 nm. This feature can also be seen in the wild-type spectrum, although it is less pronounced. At 30 ps, an absorption decrease is observed at approximately 805 nm in the LH(L131) reaction centers but not in wild-type reaction centers, while at 815 nm the absorption decrease that is predominant in the wild type is significantly reduced in the mutant. At approximately 600 ps, the spectra are similiar in the wild type and the mutant, and the bleaching at 805 nm is no longer present in the mutant.

The absorption change seen between 0.5 and 30 ps in wild-type reaction centers in the 850–960-nm region has been attributed to the decay of stimulated emission from the excited singlet state of P (Woodbury et al., 1985; Martin et al., 1986; Kirmiaer & Holten, 1988; Chan et al., 1991). Compared to the wild type, the LH(L131) reaction centers show a substantial recovery of the initial bleaching in the 820–860-nm region (Figure 5).

Less detailed time-resolved spectral measurements have been performed on the other mutants. Spectral features similar to LH(L131) reaction centers in the 720–820-nm region were observed for LH(M160) and GD(M203) reaction centers (data not shown). In the 820–860-nm region, the significant recovery observed in the LH(L131) spectra was also present in the LH(M160) spectra, but was not seen in the GD(M203)

Table III: Summary of Results on Bacteriochlorophyll 9-Keto Hydrogen Bond Mutants

strain	P/P^+ E_m[a] (mV)	$P^*/P^+H_A^-$ ΔG[b] (mV)	P^* decay time[c] (ps)	$P^+H_A^- \rightarrow P^+Q_A^-$ time[c] (ps)	$P^+Q_A^- \rightarrow PQ_A$ time[c] (ms)
wild type	495	−120	3.4	200	100
LH(L131)	575	−65	12.2	220	70
LH(M160)	550	−100	5.7	210	75
GD(M203)	495	−95	9.4	215	95
ID(L177)	470	−115	4.4	225	185

[a] Estimated error in E_m, the redox midpoint potential, is ±10 mV. [b] Calculated from several experiments, estimated error ±5 mV. [c] Estimated error ±10%.

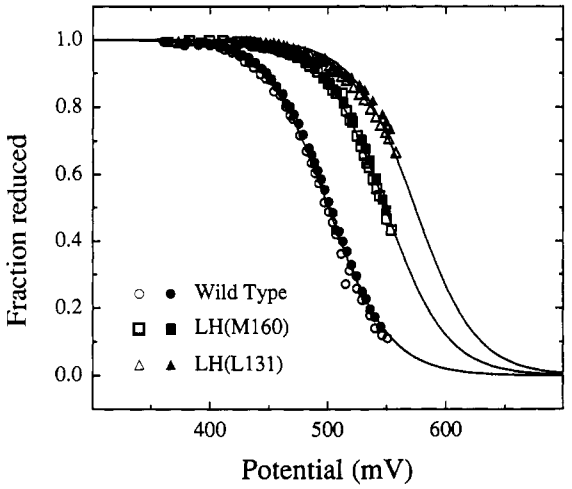

FIGURE 4: Redox titrations of reaction centers. The extent of reduction of the dimer was determined by measuring the optical absorption of the dimer peak (865 nm in the wild type), while monitoring the ambient redox potential. The open symbols represent data from an oxidative titration, and the closed symbols represent data from a subsequent reductive titration on the same sample. The solid lines depict the fits of the Nernst equation ($n = 1$) for the combined data using a single parameter, E_m, the midpoint potential. The midpoint potentials relative to the wild type increased by approximately 55 and 80 mV for the LH(M160) and LH(L131) mutants, respectively (Table III).

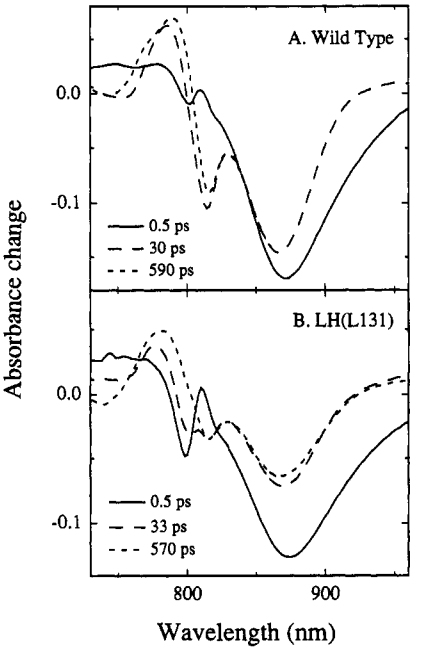

FIGURE 5: Difference absorption spectra measured for (A) wild-type reaction centers at 0.5, 30, and 590 ps after excitation at 590 nm with a 200-fs pulse, and (B) LH(L131) reaction centers at 0.5, 33, and 570 ps after excitation. For these measurements, magic angle polarization between the excitation and probe pulse was used. Excitation intensities, sample cell, and spectral resolution were as described in Taguchi et al. (1992). Additional resolved bands near 800 nm at 30 ps are observed in the mutant. The substantial absorption change in the mutant in the 820–860-nm region indicates a yield loss during electron transfer.

spectra. The spectral features of the ID(L177) mutant were similar to those of the wild type.

The kinetics of P* decay for each of the mutants were determined by monitoring the stimulated emission as a function of time (Figure 6). The absorption changes at a single wavelength, 920 nm, could be fit with a single exponential term and a constant, giving a 3.4-ps decay time for P* in the wild type and values between 4.4 and 12.2 ps for the mutants (Table III). However, the decay kinetics varied with wavelength, particularly in the LH(L131) and LH(M160) mutants. For example, the recovery of the bleaching at 860 nm had characteristic times of 8 and 21 ps for the LH(M160) and LH(L131) mutants, respectively, compared to characteristic times of approximately 5.7 and 12.2 ps for the decay of the stimulated emission at 920 nm. Analysis of the P* decay as a function of wavelength using more than one exponential term is in progress.

The recovery of the bleaching of the Bphe absorption band at 760 nm in wild-type and LH(L131) reaction centers is shown in Figure 7. Decays with similar kinetics were obtained for LH(M160), GD(M203), and ID(L177) reaction centers (data not shown). These results indicate that the rate of electron transfer from Bphe to quinone is essentially the same in the mutants as the wild type (Table III).

DISCUSSION

Four mutants are described, each containing an alteration designed to introduce a proton-donating residue that could form a hydrogen bond with the 9-keto carbonyl of one of the reaction center Bchls. The two mutants designed to affect the dimer Bchls involved changes at symmetry-related residues, Leu L131 and Leu M160. These residue positions, for which no functional role has been assigned other than being hydrophobic, are either a leucine or isoleucine in other bacterial reaction centers (Komiya et al., 1988). These residues are located in the C transmembrane helices of the reaction centers in such a way that they are adjacent to the edges of the two Bchls of the dimer, which interacts primarily with the D and E transmembrane helices (Allen et al., 1987b). In each case computer modeling indicated that formation of a hydrogen bond would be most favorable by mutation to a histidine residue, if there were no other changes in the structure. The other two mutations were designed to introduce hydrogen bonds at the monomer Bchls. However, placement of a residue in a suitable position was more difficult than for the dimer Bchls. The two residues that were selected are not symmetry related, although both are located in the D transmembrane helices.

In the low-temperature optical spectra, the dimer peak at 890 nm shifts by ~10 nm, corresponding to a shift in energy of ~125 cm^{-1}, in the two mutants near the dimer Bchls, LH-

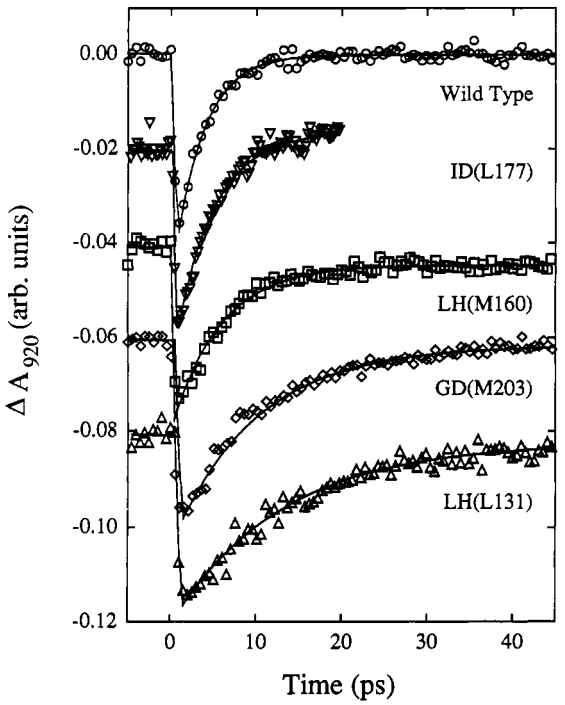

FIGURE 6: Kinetics of initial electron transfer in reaction centers. The decays of the stimulated emission of P* at 920 nm subsequent to photoexcitation at 590 nm with a 200-fs pulse are compared. The decays were deconvoluted with an appropriate instrument response function and fit to a single exponential and a constant. The solid lines depict the best fits through the curves. Wild type, ID(L177), LH(M160), GD(M203), and LH(L131) yielded lifetimes for P* of 3.4, 4.4, 5.5, 9.1, and 12.8 ps, respectively. The values shown in Table III are average values taken from a series of decays.

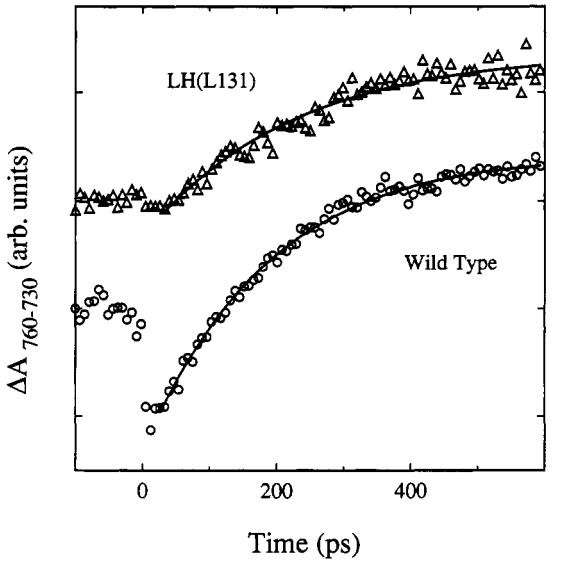

FIGURE 7: Kinetics of electron transfer from Bphe to quinone. The recoveries of the absorption changes at 760 nm in wild-type and LH(L131) reaction centers are shown. Dual wavelength (760–730 nm) absorption changes were used to correct errors due to baseline drift. Least-squares fits of the data are presented with time constants of 200 and 220 ps for wild type and LH(L131), respectively, which are equivalent within the error of the measurement. The LH(M160), GD(M203), and ID(L177) mutants have absorption changes with similar time constants (Table III).

(L131) and LH(M160). The energies of this transition moment have been calculated to shift by 50–200 cm^{-1} due to the effect of hydrogen bonds (Hanson et al., 1987; Thompson et al., 1991), consistent with the magnitude of the shifts observed in the mutants. For three of the mutants, LH(L131), LH(M160), and GD(M203), the Bchl peaks at 600 and 800 nm have more than one resolved transition in low-temperature spectra, presumably because one of the Bchls has a different electronic structure compared to the wild type due to hydrogen-bonding interactions. The difference between the Q_x bands of the Bchls in these mutants is similar to the difference between the Q_x bands of the Bphes, which is caused by the hydrogen bonding of Glu L104 (Bylina et al., 1988). Electrostatic interactions or a repositioning of the Bchls due to placing a histidine or aspartic acid residue near the Bchls may also contribute to the observed effects of these mutations.

Assignment of the light-induced absorption changes seen in the 800-nm region of the optical spectrum of wild-type reaction centers has been controversial (Holzapfel et al., 1990; Kirmaier & Holten, 1991). The specific perturbation of the transitions of the bacteriochlorophylls that absorb in the 800-nm region should facilitate the identification of transient signals. As was observed in the low-temperature steady-state absorption spectra, additional resolved transitions are evident in difference spectra on the picosecond time scale of LH(L131), LH(M160), and GD(M203) reaction centers. Comparison of the wild-type and LH(L131) difference absorption spectra shows substantial differences in the 800-nm region (Figure 5). At 0.5 ps, a substantial bleaching in the 800-nm region is seen in both wild type and LH(L131), although this feature is blue-shifted by approximately 5 nm in the mutant. This bleaching presumably arises from the involvement of the state B* at early times due to the 590-nm excitation of all bacteriochlorophylls in the system, since this feature is not observed when 860 nm excitation of wild-type reaction centers is used [e.g., Kirmaier et al. (1991)]. By 30 ps, P* decay is nearly complete, and the state formed at this time clearly has different spectral properties in the wild-type and LH(L131) reaction centers. The distinct bleaching at approximately 805 nm in the LH(L131) mutant is not seen in wild type. The differences between the wild-type and LH(L131) spectra largely dissappear by 600 ps. The spectral differences indicate either the presence of a new electronic state in LH(L131) reaction centers or an electronic transition that is present but not resolved in the wild type. It is not clear whether these additional absorption changes represent either involvement of B_A or B_B in electron transfer or changes in the spectral characteristics of $P^+H_A^-$. Further analysis of these spectra as a function of temperature and additional measurements in the Bchl/Bphe anion absorption region (620–700 nm) should help clarify the involvement of B_A or B_B in the 30-ps transient state.

Significant differences between wild-type and LH(L131) reaction centers are also observed on the picosecond time scale in the 820–960-nm region (Figure 5). The mutant shows a much larger recovery of the bleaching than the wild type in the 820–860-nm region, indicating a yield loss during the initial charge separation event. Assuming no changes in the absorption spectrum of either P* or the initial charge separated state in the mutant, then the magnitude of the ground-state recovery leads to a yield estimate for the initial charge separation of 70%. A similar yield loss has been estimated for LH(M160) reaction centers. The lower yield of initial charge separation in the heterodimer mutants has been postulated to be due to an increased contribution from charge-transfer states in P* (Kirmaier et al., 1988, 1989), which can couple the ground and excited states of P electronically (Warshel et al., 1988). The addition of a hydrogen bond to P_A and P_B in LH(L131) and LH(M160) reaction centers, respectively, may similarly perturb the symmetry of P sufficiently to increase the charge-transfer character of P*.

Alternatively, the yield loss in the mutants may be due a distinct population of reaction centers in which P* decays rapidly but no charge separation occurs. The observed wavelength dependence of the kinetics of the absorption changes between 850 and 920 nm is consistent with the presence of more than one species of P*.

The P/P^+ redox midpoint potentials were observed to be higher in the LH(L131) and LH(M160) mutants than in the wild type. Increasing the P/P^+ midpoint potential should decrease the free energy difference between P* and the states $P^+B_A^-$, $P^+H_A^-$, and $P^+Q_A^-$ since shifts in the energy of the P to P* transition in these mutants are less than 25 meV. If electron transfer to Q_A is blocked by chemical reduction of the quinone, $P^+H_A^-$ is stable for nanoseconds in wild-type reaction centers. Under these conditions, long-lived fluorescence components that have small amplitudes compared to the prompt component result from the low population of P* that remains after the reaction $P^* \leftrightarrow P^+H_A^-$ has equilibrated. An increase is observed in the amplitude of the long-lived fluorescence components of the two mutants, LH(L131) and LH(M160), that show the greatest increase in the P/P^+ midpoint potential, indicating that the $P^*/P^+H_A^-$ energy difference has decreased.

A standard free energy gap between P* and $P^+H_A^-$ can be estimated from the transient fluorescence data, although this calculation is model dependent (Schenck et al., 1982; Woodbury & Parson, 1984; Taguchi et al., 1992). In the LH(L131) and LH(M160) mutants, an increase in the P/P^+ midpoint potential is correlated with a decrease in the calculated $P^*/P^+H_A^-$ free energy difference (Table III). However, the decreases in the free energy gaps calculated for the mutants are not as large as would be expected from the increases in the P/P^+ midpoint potentials. The discrepancy between changes in calculated free energy gaps and changes in P/P^+ midpoint potentials may arise for several reasons (Taguchi et al., 1992; Stocker et al., 1992). In addition to differences between the species being measured in the two experiments ($P^+H_A^-$ compared to P^+) and the time scales of the measurements (picoseconds compared to minutes), inherent inaccuracies exist in the estimation of the free energy difference due to the limited time resolution of the time-correlated single photon counting apparatus. The actual P* lifetime is determined from separate measurements of stimulated emission decay in reaction centers under nonreducing conditions and is fit to a single exponential. Quinone reduction has been shown to result in a small increase (~30%) in the lifetime of P* (Woodbury et al., 1985) in wild-type reaction centers and may also have similar effects on the lifetime in the mutants. Deviations from strict exponential decay will also have a quantitative effect on the correction of the P* lifetime and amplitude used in the ΔG calculations. Thus, while a qualitative correlation would be expected between the P/P^+ midpoint potential and the calculated free energy difference between P* and $P^+H_A^-$, a direct correspondence may not necessarily be found.

The correlation between the P/P^+ midpoint potential and the calculated free energy gap between P* and $P^+H_A^-$ does not extend to the GD(M203) mutant (Table III). For this mutant there is essentially no change in the midpoint potential but a decrease of 25 mV in the calculated free energy gap, compared to the calculated free energy gap of 120 mV for the wild type. Since GD(M203) was designed to alter B_A and not P, it is not surprising that there is little change in the P/P^+ midpoint potential compared to wild type. The calculated free energy difference for the GD(M203) mutant is smaller than the wild type due to an increase in the amplitude of the 100-ps component, A_2, of the fluorescence decay (Table II). No significant increase is observed in the amplitudes of the slower components, A_3 and A_4, in contrast to the large increases observed for all three long-lived components in the LH(L131) and LH(M160) mutants. The 100-ps component has the same fluorescence spectrum as the other components, indicating that it does arise from P*. The lack of a uniform increase in the amplitudes of all three long-lived components in the GD(M203) mutant suggests that the fluorescence decay on the 100-ps time scale may not represent an equilibrated state between P* and $P^+H_A^-$. Excluding this component, A_2, from the free energy calculation yields a value for the energy difference in the GD(M203) mutant that is closer to the wild type than that calculated using all components. A similar calculation for the LH(M160) and LH(L131) mutants results in a decrease in the estimated free energy difference that is larger than that obtained using all three long-lived component amplitudes.

Alteration of the free energies of the states $P^+B_A^-$, $P^+H_A^-$, and $P^+Q_A^-$ relative to P* and the ground state should change the rate of the initial charge separation and the rate of charge recombination from Q_A^-. For the mutants designed to alter the dimer, LH(L131) and LH(M160), driving forces for electron transfer to H_A are decreased relative to wild type. The P* decay times for these mutants are slower than wild type, with the slowest rate being found for LH(L131), the mutant with the smallest calculated ΔG. A correlation is also observed between the P/P^+ midpoint potential and the rate of $P^+Q_A^-$ charge recombination. Each of the mutants that had an increased P/P^+ potential showed a faster decay rate for $P^+Q_A^-$. The ID(L177) mutant, which had a decreased P/P^+ oxidation potential, showed a decreased decay rate for $P^+Q_A^-$, although the magnitude of the decrease is much larger than might be expected from the relatively small potential change. These correlations suggest that for these two reactions, smaller driving forces result in slower electron-transfer rates.

The general effect of slower initial electron-transfer rates being associated with smaller driving forces has been observed in other mutants with changes near the Bchl cofactors. The heterodimer mutants, in which changes in Mg^{2+} ligands result in Bchl–Bphe exchanges at P, show increased P/P^+ redox potentials and slower initial electron-transfer rates (Kirmaier et al., 1988; Schenck et al., 1990). The two dimer hydrogen bond mutants, LH(L131) and LH(M160), are similar to the heterodimer mutants in that, for both of these types of mutations, the major effect is that one Bchl of the dimer has been perturbed relative to the other. A mutant of *Rhodobacter capsulatus* with large scale changes involving exchanges of sections of the L and M genes also shows an increased P/P^+ redox potential, a smaller calculated $P^*/P^+H_A^-$ energy difference, and a slower initial electron-transfer rate (Woodbury et al., 1990; Taguchi et al., 1992).

The GD(M203) mutant was designed to alter the electronic states of B_A. Based upon the results of the LH(L131) and LH(M160) mutants, the formation of a hydrogen bond with B_A in the GD(M203) mutant should decrease the reduction potential of B_A and, consequently, decrease the free energy of $P^+B_A^-$ relative to $P^+H_A^-$. The mutation M210 Tyr to Phe is thought to increase the energy of the state $P^+B_A^-$ (Nagarajan et al., 1990; Parson et al., 1990; Finkele et al., 1990; Chan et al., 1991; Middendorf et al., 1991). Both the GD(M203) mutant, which should decrease the $P^+B_A^-$ free energy, and the M210 Tyr to Phe mutant, which is thought to increase the $P^+B_A^-$ free energy, result in a similar decrease in the rate of

initial electron transfer. Assuming these mutations are primarily affecting electron-transfer rates by altering the energy of $P^+B_A^-$ and not the electronic coupling between P and B_A, then the free energy of $P^+B_A^-$ in wild-type reaction centers is apparently set to optimize the rate of electron transfer.

The ID(L177) mutant is clearly different from the other three mutants. In low-temperature absorption spectra, the splittings of the peaks observed in the other mutants are not present, and the 800-nm peak is more symmetrical than in the wild type. An increase of approximately 25 meV in the P/P^* energy difference is indicated by the shift of the P absorption band. Unlike the other mutants, the P/P^+ midpoint potential is slightly lower than the wild type. These changes are not consistent with the small decrease in the calculated $P^*/P^+H_A^-$ free energy difference. The effects of this mutation do not appear to be due to the formation of a hydrogen bond to B_B and may arise from structural changes or electrostatic interactions.

The changes in steady-state and time-resolved optical spectra of the LH(M160), LH(L131), and GD(M203) mutants are consistent with a perturbation of the electronic structure of the dimer due to the formation of a hydrogen bond. In light-induced Fourier transform infrared difference spectra of the LH(M160) and LH(L131) mutants, changes in both amplitudes and frequencies of the differential signals indicate a significant perturbation of the environment of the 9-keto groups of P, which has been attributed to the formation of hydrogen bonds (Nabedryk et al., 1992). Electron nuclear double resonance spectra of the LH(M160) and LH(L131) mutants have lines shifted compared to the wild type. Preliminary analysis of these spectra indicates that the spin density distribution in P^+ is altered by asymmetrical hydrogen bonding in the mutants (Rautter et al., 1992). The putative hydrogen bonds in these mutants are correlated with the modulation of the oxidation–reduction potentials of the Bchls and corresponding changes in the electron-transfer rates, demonstrating that specific interactions between proteins and Bchls, such as hydrogen bonds, have predictable effects on the properties of Bchls.

ACKNOWLEDGMENT

We wish to thank V. H. Coryell and X. Zhang for assistance with the preparation of the reaction centers.

REFERENCES

Allen, J. P., Feher, G., Yeates, T. O., Komiya, H., & Rees, D. C. (1987a) *Proc. Natl. Acad. Sci. U.S.A. 84*, 5730–5734.

Allen, J. P., Feher, G., Yeates, T. O., Komiya, H., & Rees, D. C. (1987b) *Proc. Natl. Acad. Sci. U.S.A. 84*, 6162–6166.

Bylina, E. J., Kirmaier, C., McDowell, L., Holten, D., & Youvan, D. C. (1988) *Nature 336*, 182–184.

Chan, C.-K., Chen, L. X.-Q., DiMagno, T. J., Hanson, D. K., Nance, S. L., Schiffer, M., Norris, J. R., & Fleming, G. R. (1991) *Chem. Phys. Lett. 176*, 366–372.

Coleman, W. J., & Youvan, D. C. (1990) *Annu. Rev. Biophys. Biophys. Chem. 19*, 333–367.

Ditta, G., Schmidhauser, T., Yakobson, E., Lu, P., Liang, X.-W., Finlay, D. R., Guiney, D., & Helinski, D. R. (1985) *Plasmid 13*, 149–153.

Farchaus, J. W., & Oesterhelt, D. (1989) *EMBO J. 8*, 47–54.

Feher, G., Arno, T. R., & Okamura, M. Y. (1988) in *The Photosynthetic Bacterial Reaction Center* (Breton, J., & Vermeglio, A., Eds.) pp 271–287, Plenum, New York.

Feher, G., Allen, J. P., Okamura, M. Y., & Rees, D. C. (1989) *Nature 339*, 111–116.

Finkele, U., Lauterwasser, C., Zinth, W., Gray, K. A., & Oesterhelt, D. (1990) *Biochemistry 29*, 8517–8521.

Franzen, S., Goldstein, R. F., & Boxer, S. G. (1990) *J. Phys. Chem. 94*, 5135–5149.

Gunner, M. R., & Dutton, P. L. (1989) *J. Am. Chem. Soc. 111*, 3400–3412.

Gust, D., Moore, T. A., Luttrull, D. K., Seely, G. R., Bittersmann, E., Bensasson, R. V., Rougée, M., Land, E. J., De Schryver, F. C., & Van der Auweraer, M. (1990) *Photochem. Photobiol. 51*, 419–426.

Hanson, L. K., Thompson, M. A., & Fajer, J. (1987) in *Progress in Photosynthesis Research* (Biggens, J., Ed.) Vol. I, pp 311–314, Martinus Nijhoff, Dordrecht.

Holzapfel, W., Finkele, U., Kaiser, W., Oesterhelt, D., Scheer, H., Stilz, H. U., & Zinth, W. (1990) *Proc. Natl. Acad. Sci. U.S.A. 87*, 5168–5172.

Kiley, P. J., & Kaplan, S. (1988) *Microbiol. Rev. 52*, 50–69.

Kirmaier, C., & Holten, D. (1987) *Photosynth. Res. 13*, 225–260.

Kirmaier, C., & Holten, D. (1988) *Isr. J. Chem. 28*, 79–85.

Kirmaier, C., & Holten, D. (1991) *Biochemistry 30*, 609–613.

Kirmaier, C., Holten, D., Bylina, E. J., & Youvan, D. C. (1988) *Proc. Natl. Acad. Sci. U.S.A. 85*, 7562–7566.

Kirmaier, C., Bylina, E. J., Youvan, D. C., & Holten, D. (1989) *Chem. Phys. Lett. 159*, 251–257.

Kirmaier, C., Gaul, D., DeBey, R., Holten, D., & Schenck, C. C. (1991) *Science 251*, 922–927.

Komiya, H., Yeates, T. O., Rees, D. C., Allen, J. P., & Feher, G. (1988) *Proc. Natl. Acad. Sci. U.S.A. 85*, 9012–9016.

Martin, J.-L., Breton, J., Hoff, A. J., Migus, A., & Antonetti, A. (1986) *Proc. Natl. Acad. Sci. U.S.A. 83*, 957–961.

Middendorf, T. R., Mazzola, L. T., Gaul, D. F., Schenck, C. C., & Boxer, S. G. (1991) *J. Phys. Chem. 95*, 10142–10151.

Moore, G. R., & Pettigrew, G. W. (1990) *Cytochromes c*, Springer-Verlag, Berlin.

Moss, D. A., Leonhard, M., Bauscher, M., & Mäntele, W. (1991) *FEBS Lett. 283*, 33–36.

Nabedryk, E., Breton, J., Allen, J., Murchison, H., Taguchi, A., Williams, J., & Woodbury, N. (1992) in *The Photosynthetic Bacterial Reaction Centre: Structure, Spectroscopy, and Dynamics* (Breton, J., Ed.) Plenum, New York (in press).

Nagarajan, V., Parson, W. W., Gaul, D., & Schenck, C. (1990) *Proc. Natl. Acad. Sci. U.S.A. 87*, 7888–7892.

O'Reilly, J. E. (1973) *Biochim. Biophys. Acta 292*, 509–515.

Paddock, M. L., Rongey, S. H., Feher, G., & Okamura, M. Y. (1989) *Proc. Natl. Acad. Sci. U.S.A. 86*, 6602–6606.

Parson, W. W. (1991) in *Chlorophylls* (Scheer, H., Ed.) pp 1153–1180, CRC Press, Boca Raton.

Parson, W. W., Chu, Z.-T., & Warshel, A. (1990) *Biochim. Biophys. Acta 1017*, 251–272.

Popovic, Z. D., Kovacs, G. J., Vincett, P. S., Alegria, G., & Dutton, P. L. (1986) *Chem. Phys. 110*, 227–237.

Poulos, T. L. (1987) *Adv. Inorg. Biochem. 7*, 1–36.

Rautter, J., Gessner, Ch., Lendzian, F., Lubitz, W., Williams, J. C., Murchison, H. A., Wang, S., Woodbury, N. W., & Allen, J. P. (1992) in *The Photosynthetic Bacterial Reaction Centre: Structure, Spectroscopy, and Dynamics* (Breton, J., Ed.) Plenum, New York (in press).

Sayers, J. R., Schmidt, W., & Eckstein, F. (1988) *Nucleic Acids Res. 16*, 791–802.

Schenck, C. C., Blankenship, R. E., & Parson, W. W. (1982) *Biochim. Biophys. Acta 680*, 44–59.

Schenck, C. C., Gaul, D., Steffen, M., Boxer, S. G., McDowell, L., Kirmaier, C., & Holten, D. (1990) in *Reaction Centers of Photosynthetic Bacteria* (Michel-Beyerle, M. E., Ed.) pp 229–238, Springer-Verlag, Berlin.

Scolnik, P. A., & Marrs, B. L. (1987) *Annu. Rev. Microbiol. 41*, 703–726.

Stocker, J. W., Taguchi, A. K. W., Murchison, H. A., Woodbury, N. W., & Boxer, S. G. (1992) *Biochemistry 32*, 10356–10362.

Taguchi, A. K. W., Stocker, J. W., Alden, R. G., Causgrove, T. P., Peloquin, J. M., Boxer, S. G., & Woodbury, N. W. (1992) *Biochemistry 31*, 10345–10355.

Takahashi, E., Maroti, P., & Wraight, C. A. (1990) in *Current Research in Photosynthesis* (Baltscheffsky, M., Ed.) Vol. I, pp 169–172, Kluwer Academic Publishers, Boston.

Thompson, M. A., Zerner, M. C., & Fajer, J. (1991) *J. Phys. Chem. 95*, 5693–5700.

Tsurushita, N., Maki, H., & Korn, L. J. (1988) *Gene 62*, 135–139.

Warshel, A., Creighton, S., & Parson, W. W. (1988) *J. Phys. Chem. 92*, 2696–2701.

Woodbury, N. W. T., & Parson, W. W. (1984) *Biochim. Biophys. Acta 767*, 345–361.

Woodbury, N. W., Becker, M., Middendorf, D., & Parson, W. W. (1985) *Biochemistry 24*, 7516–7521.

Woodbury, N. W., Taguchi, A. K., Stocker, J. W., & Boxer, S. G. (1990) in *Reaction Centers of Photosynthetic Bacteria* (Michel-Beyerle, M. E., Ed.) pp 303–312, Springer-Verlag, Berlin.

Yanisch-Perron, C., Vieira, J., & Messing, J. (1985) *Gene 33*, 103–119.

Yeates, T. O., Komiya, H., Chirino, A., Rees, D. C., Allen, J. P., & Feher, G. (1988) *Proc. Natl. Acad. Sci. U.S.A. 85*, 7993–7997.

Youvan, D. C., Ismail, S., & Bylina, E. J. (1985) *Gene 38*, 19–30.